PCCP

Accepted Manuscript

ROYAL SOCIETY OF CHEMISTRY

www.rsc.org/pccp

Investigation of ESIPT in a panel of chromophores presenting N-H···N intramolecular hydrogen bonds

Pierre O. Hubin,[a]* Adèle D. Laurent,[b] Daniel P. Vercauteren,[a] Denis Jacquemin[b,c]*

Abstract

Thermodynamic and kinetic aspects of excited state intramolecular proton transfer (ESIPT) are investigated in 11 chromophores harboring an intramolecular N-H···N hydrogen bond [pyridyl pyrazoles, pyridyl pyrrole, azaindole, pyridyl indole, pyrroloquinoline, and an analogue of the Blue Fluorescent Protein (BFP) chromophore] with the help of quantum mechanical calculations. For pyridyl pyrazoles, simulated spectra are used to help the interpretation of experimental ones and the effects of several substituents are investigated. Then it is shown that Time-Dependent Density Functional Theory fails to satisfactorily describe energetic aspects of ESIPT for the BFP chromophore analogue. Equation-of-Motion Coupled Cluster theory is thus used to reach accurate insights for that challenging case.

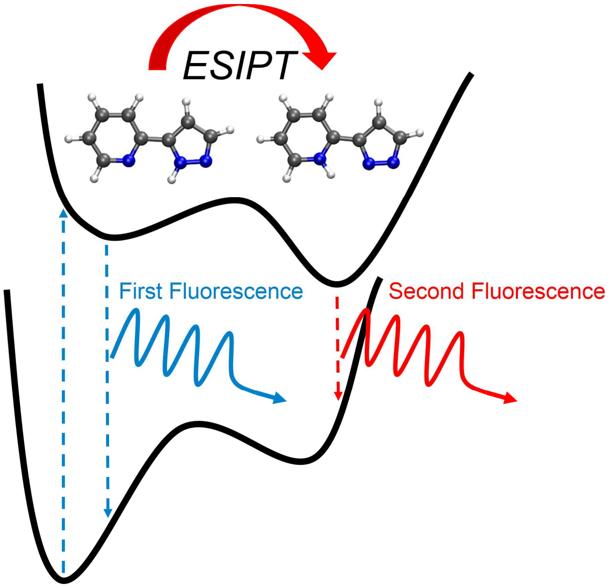

Introduction

Chromophores that undergo an excited state intramolecular proton transfer (ESIPT) have drawn much attention in the recent years.[1-10] The particularity of these compounds is that the most stable tautomeric form differs in the ground state (GS) and in the first electronically excited state (ES). As a consequence, the electronic excitation of such molecule may induce an intramolecular proton transfer (PT) associated with a large geometrical reorganization subsequently yielding a substantial Stoke shift. A typical feature of molecules undergoing ESIPT is the presence of a strong intramolecular hydrogen bond (HB). A wide panel of HB acceptors and donors has been reported in literature,[4-6,9-11] and several have been used to build ESIPT dyes. More precisely hydroxyphenyl benzotriazole (BZT),[4] hydroxyphenyl benzothiazole (HBT),[5] hydroxyphenylimidazopyridine (HPIP),[10] and hydroxyphenylbenzoxazole (HBO)[11] structures are amongst the hallmark ESIPT structures. These are all O-H···N systems containing intramolecular HB forming 6-membered ring. An analogue of the Green Fluorescent Protein (GFP) chromophore harboring a 7-membered ring O-H···N HB has also been reported.[6] In the present work, we focus on compounds containing nitrogen atoms as both donor and acceptor moieties (N-H···N) and, more specifically, we give an emphasis to pyridyl pyrazoles (**1a-f**, see Fig. 1). The emission spectra of such compounds show two fluorescent bands, the first is nearly the mirror-image of the absorption and is attributed to emission from the canonical form (N), whereas the second, displaced at much larger wavelengths, is a signature of the proton-transferred tautomeric isomer (T).[12] It appears that subtle changes in the structure of this family of molecules may induce important changes in the PT mechanism (both intra and/or intermolecular in protic media) and consequently tune their emission spectra.[13-15] We here investigate these phenomena on the basis of *ab initio* calculations, including both Time-Dependent Density Functional Theory (TD-

DFT) and Equation-of-Motion Coupled Cluster (EOM-CC) approaches. In order to reach a better understanding of pyridyl pyrazole chromophores we compare them with several other N-H¨N systems (pyridyl pyrrole **2**,[16,17] azaindole **3**,[18-22] pyridyl indole **4**,[23-25] and pyrroloquinoline **5**[26,27]) for which experimental,[16,18,24,26] as well as theoretical studies were published previously.[17,19-23,25-27] Interestingly, these N-H¨N chromophores display different behaviors upon excitation. For instance, the fluorescence spectrum of **2** in apolar solvents exhibits two fluorescent bands. The second band, characterized by a very large Stoke shift, presents a small intensity compared to the main band, and this situation also holds for **1**. Thanks to Complete Active Space Self-Consistent Field (CASSCF) calculations, Sobolewski and co-workers showed that the presence of a Conical Intersection (CI) on the Potential Energy Surface (PES) of the T form leading to a non-radiative interconversion explains the elusive character of this band in **2**.[17] The ESIPT phenomenon was also studied with theoretical tools for molecule **4**, notably Multi-State Complete Active Space Second-Order Perturbation Theory (MS-CASPT2) and OM2/Multireference Configuration Interaction (MRCI) nonadiabatic dynamics simulations.[25] It appeared that in **4** the ESIPT phenomenon is very fast, but again it is followed by a non-radiative relaxation through a CI.[23,25] For this reason, the second fluorescence is not observed in this molecule. In both **3** and **5**, previous theoretical works, based on TD-DFT, CASSCF, and CASPT2, showed that the energy barrier for ESIPT is relatively high.[19-22,26,27] The PT in the ES can still take place intermolecularly through dimerization of **3**,[19,21] and *via* the participation of a protic solvent molecule interacting with **3** and **5**.[20,22,26,27] The effects of substituents in position 3 of chromophore **1** (see Fig. 1 for atom numbering) have been recently studied experimentally.[14] It was proposed that an electro-withdrawing group (EWG) as –CF_3 lowers the ESIPT barrier resulting in a strong increase of the second emission band.[14] To the best of our knowledge, this interesting substituent effect in molecules **1a-c** has not been investigated with a theoretical approach yet. Such task is performed in the present study using simulated spectra to help interpreting the experimental ones. In addition, on the contrary to previous reports involving molecule **1**, the analysis is here based on both ES and GS optimized structures and solvents effects are taken into account as well (see Computational Methods section for details). We also provide a closer look on the impact of substituents on ESIPT in pyridyl pyrazoles by comparing the relative stabilities between N and T forms, as well as energy barriers for the PT in molecules **1a-f**. Chromophores with acceptor and donor groups on both pyrazole and pyridyl moieties are considered as depicted in Fig. 1. We also report, for the first time, vibrationally-resolved spectra for key dyes. At last, we focus on an analogue of the Blue Fluorescent Protein (BFP) chromophore **6** in which the ESIPT phenomenon has recently been proposed to explain its particular fluorescence spectrum.[28] The structures of all studied molecules are presented in Fig. 1.

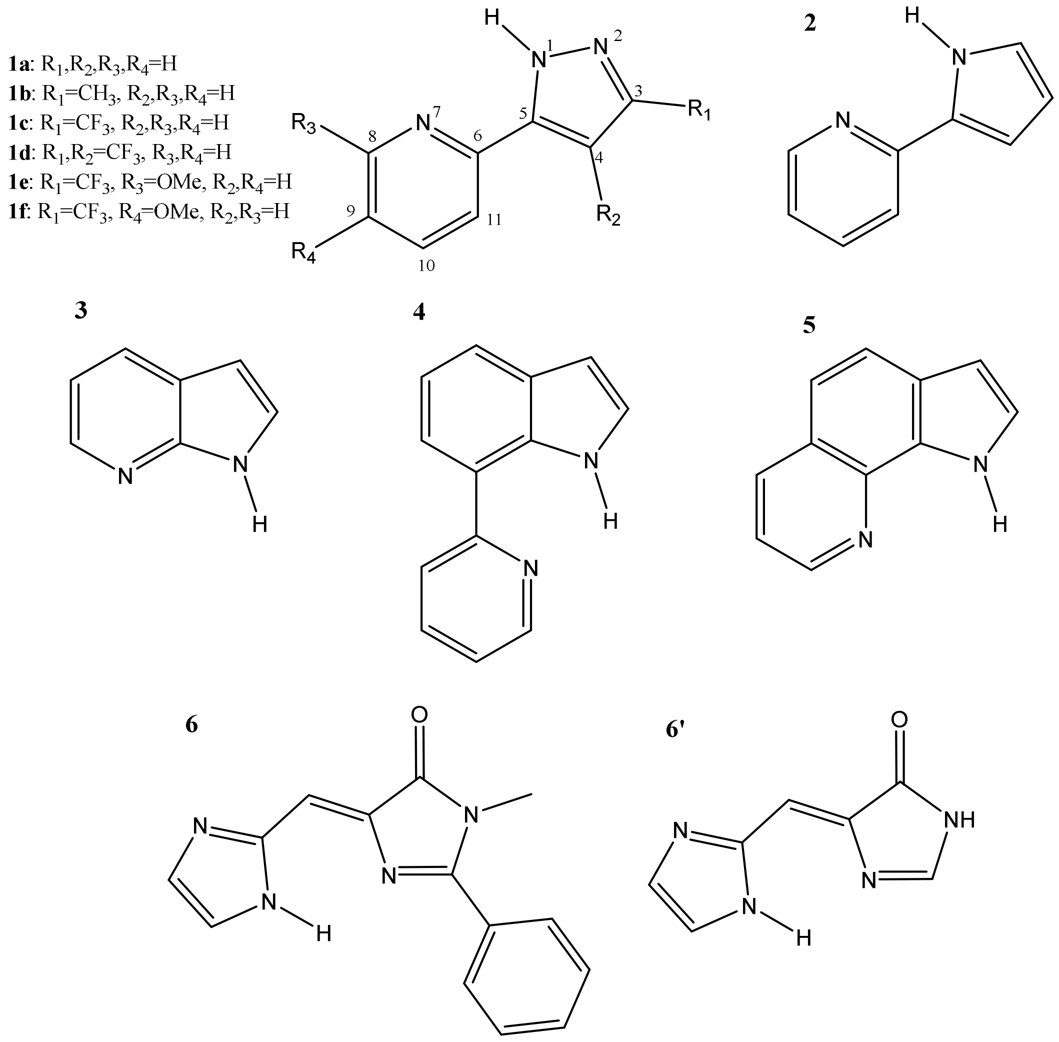

Fig. 1 Planar structures of the studied molecules. **1a-f**: pyridyl pyrazoles, **2**: pyridyl pyrrole, **3**: azaindole, **4**: pyridyl indole, **5**: pyrroloquinoline, **6**, **6'**: BFP chromophore analogue.

Computational Details

All calculations were performed with Gaussian09.[29] The ground and excited state geometries have been optimized at the DFT and TD-DFT levels of theory, respectively. To achieve numerically stable and accurate values, we have tightened the self-consistent field (10^{-10} *a.u.*) and geometry optimization (10^{-5} *a.u.*) convergence thresholds, as well as used a (99,590) pruned DFT integration grid (so-called *ultrafine* grid). We have selected the M06-2X functional[30] to carry out our calculations, a choice justified by numerous previous benchmarks demonstrating the accuracy of this functional for predicting both vertical and adiabatic transition energies as well as for predicting band shapes.[31-34] Vibrational frequencies were next computed for each stationary point to confirm it corresponds to a minimum, no imaginary frequency, or a Transition State (TS), one imaginary frequency. It is worth pointing out that locating the ES TS requires several computational steps. Here we used the adequate Berny algorithm and did not relied on "simple" scans of the ES PES nor on approximated vertical TD-DFT calculations performed on the GS TS. All these structural calculations employed the 6-31+G(d) atomic basis set that includes both polarization and diffuse functions. Transition energies (absorption and emission), were computed with a much larger 6-311++G(2df,2p) atomic basis set. For molecules **1a**, **1c**, **2,** and **6**, EOM-CCSD calculations were carried out using DFT/TD-DFT optimized structures. Environmental effects were considered using the well-known PCM model.[35] While geometry DFT optimizations and Hessian have been determined with the popular linear-response (LR) PCM approach to account for solvation effects on both ground and excited states; all excited state and transition energies have been obtained using the corrected LR scheme (cLR).[36,37] The cLR model allows correcting the cavity polarization by accounting for the change of electron density upon electronic transition. Therefore, it allows not only to compare structures having different variations of dipole moment amplitudes between the ground and excited states but also to estimate emission wavelengths (and hence Stokes shifts) with more accuracy. Of course, while we applied the equilibrium PCM limit for optimization and vibrational TD-DFT calculations (slow phenomena), absorption and fluorescence wavelengths are corrected for non-equilibrium effects (fast phenomena). EOM-CCSD calculations have been performed in gas-phase as PCM-EOM-CCSD are not implemented in Gaussian09. Vibrationnaly resolved spectra have been obtained using the FCclasses program.[38-40] The reported spectra have been simulated using convoluting Gaussian functions presenting a half width at half maximum adjusted to allow accurate comparison with experiments. The Franck-Condon approximation has been employed. 0-0 energies that are represented in Fig. 2 have been computed following the procedure described in Ref. 32.

Results and Discussion

In this paragraph we first assess the accuracy of the TD-DFT approach on the basis of comparisons with both EOM-CCSD benchmarks and experimental data. Then an investigation of ESIPT in the eight considered molecules is made considering both thermodynamic and kinetic aspects. In a last part we compare experimental spectra with vibrationnaly resolved calculations.

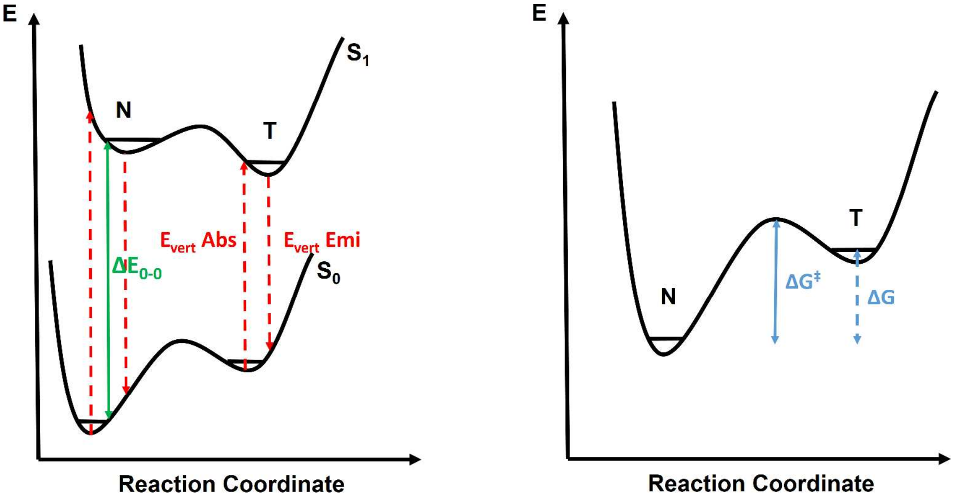

Fig. 2 Representation of key energetic values in the ESIPT process, the reaction coordinate corresponds to the PT. Dashed red arrows represent vertical transition energies (E_{vert} Abs, E_{vert} Emi), the green double arrow the 0-0 energy ($\Delta E_{0\text{-}0}$), the blue arrow is the free energy barrier ($\Delta G^{‡}$), whereas its dashed counterpart is the free energy difference between N and T forms (ΔG).

Assessment of the theoretical method

We first benchmark the performances of TD-DFT for the studied molecules on the basis of both theoretical and experimental references. In Table 1, the TD-DFT values are compared to EOM-CCSD data. TD-DFT reproduces well spectroscopic values with a Mean Unsigned Error (MUE) of 0.12 eV. The chosen functional (M06-2X) also provides a very reasonable estimate for the relative stabilities of the two tautomers (ΔE) and the corresponding energy barriers ($\Delta E^{‡}$) with a

MUE of 0.09 eV for all these data. It is worth noticing that the relative stability between N and T isomers in the ES for molecule **6** is the only case where TD-DFT fails to reproduce the EOM-CCSD trend. This case will be discussed separately in the following (see below).

Table 1 Vertical absorption and emission energies (in eV) computed for the canonical (N) and tautomeric (T) isomers, as well as relative stabilities (ΔE, T *versus* N, in eV) and energetic barriers ($\Delta E^{\ddagger}$, from N to the TS, in eV) for the ESIPT process computed with the M06-2X functional in vacuum. Values computed at the EOM-CCSD level are given in parentheses. Results are obtained with 6-311+G(2d,p) as atomic basis set for molecules **1a**, **1c**, and **2**, and with 6-31+G(d) for molecule **6**.

	E_{vert} Abs N	E_{vert} Abs T	E_{vert} Emi N	E_{vert} Emi T
1a	4.84 (4.82)	3.29 (3.25)	4.23 (4.34)	2.41 (2.54)
1c	4.92[a]	3.44[a]	4.31 (4.41)	2.72 (2.78)
2	4.44 (4.56)	3.17 (3.17)	3.91 (4.04)	2.24 (2.35)
6	3.46 (3.80)	2.82 (2.74)	2.83 (3.14)	2.46 (2.39)
	ΔE (GS)	ΔE (ES)	$\Delta E^{\ddagger}$ (GS)	$\Delta E^{\ddagger}$ (ES)
1a	1.09 (1.15)	-0.56 (-0.50)	1.36 (1.47)	0.38 (0.47)
1c	0.95[a]	-0.57 (-0.54)	1.25[a]	0.41 (0.47)
2	0.83 (0.87)	-0.63 (-0.59)	1.18 (1.30)	0.26 (0.33)
6	0.69 (0.81)	0.18 (-0.10)	0.82 (1.03)	0.33 (0.30)

[a] EOM-CCSD calculations were not performed for the GS of molecule **1c**.

Experimental and theoretical spectroscopic data obtained for molecules **1a**-**c** and **2** are compared in Table 2. The absorption and emission energies for the N isomer, as well as the 0-0 energies, corresponding to the crossing point between absorption and emission curves ($E_{0\text{-}0}$), are all well described by TD-DFT despite a slight overestimation (MUE=0.33 eV), typical of M06-2X.[31,32,34] We note that this error falls to 0.23 eV if we only consider 0-0 energies and this error is probably more significant, as 0-0 energies allow well-grounded comparisons with experimental values.[32] We also note that the redshift observed when going from **1** to **2** is well reproduced by TD-DFT. For the T isomers, there is no available absorption data and the experimentally reported fluorescence bands are both extremely broad and weakly intense in these molecules, making straightforward theory-experiment comparisons difficult. For instance in **1a**, the relative intensity of T compared to N emission is only around 2% and the fluorescence spans from 1.77 to 2.25 eV.[14] Nevertheless, we note a systematic overshooting of the emission energies and, consequently, an undershooting of the Stokes shifts. A more in-depth comparison to experimental spectroscopic data based on vibronic spectra for molecules **1a** and **1c** is available below.

Table 2 Excitation energies (in eV) and Stoke shifts (in cm^{-1}) computed with the M06-2X functional using the vertical TD-DFT approximation. 0-0 energies computed with TD-DFT are listed as well. Effects of bulk solvation (cyclohexane) are modeled with the cLR-PCM method. Experimental values, estimated from spectra,[14,18,26,28,41,42] are given in parentheses. Stokes shifts of the T form are determined using the absorption of the N isomer as reference, as there is no available experimental data for the absorption of T.

	E_{vert} Abs N	E_{vert} Emi N	E_{vert} Emi T	Stoke shift N	Stoke shift T	E_{0-0}
1a	4.79 (4.28)	4.12 (3.76)	2.80 (1.77-2.25)	4180 (5293)	15973 (18125)	4.35 (4.13)
1b	4.75 (4.28)	4.07 (3.76)	2.60 (1.77-2.25)	4180 (5495)	17323 (18125)	4.31 (4.13)
1c	4.86 (4.28)	4.19 (3.87)	3.05 (2.43-2.82)	3240 (5502)	14658 (12504)	4.43 (4.13)
2	4.35 (4.00-4.28)	3.81 (3.44-3.65)	2.52 (1.88-2.30)	3700 (4276)	14748 (15500)	3.99 (3.76)

Investigation of the ESIPT mechanism along the N-H¨N HB pattern

The relative energies between the N and T forms as well as the PT energy barriers in both the ground and excited states are listed for all molecules in Table 3. First it is seen that the N form is systematically thermodynamically favored in the GS, with very large barriers to reach T. In other words, only the N form is present in the GS, which is consistent with all available experimental evidences. On the contrary, the T isomer is systematically the most stable in the

ES, the only exception being the BFP chromophore analogue, **6**, for which TD-DFT predicts the PT to be unfavorable on the ES PES, a fact denied by EOM-CCSD (see below for a specific discussion of the BFP case). For all systems the energy barriers are much lower in the ES than in the GS; however a substantial energy barrier of at least 0.23 eV still exists in all investigated cases except for the pyridil indole (**4**) where the computed barrier is trifling (0.02 eV). This contrasts with the situation found in many other chromophores in which the ESIPT is described as (nearly) barrierless. For instance, the ESIPT in HBO dyes which takes place along an intramolecular O-H···N HB was recently investigated with a similar theoretical approach and energy barriers of 0.02 to 0.06 eV were found for two large compounds.[11] This is qualitiatively understandable from the nature of the N-H···N HB which is relatively weak compared to its O-H···N or O-H···O counterparts. On the basis of the large barriers computed in **3** and **5**, one can nearly dismiss the ESIPT possibility in these systems. As previously stated, in these compounds the PT is more likely to occur through dimerization or through the mediation of a protic solvent molecule.[18-22,26,27] On the basis of the imaginary frequencies computed for the ES TS, semi-classical tunneling effects have been estimated as described in Ref. 43. We observe that they are not negligible, with significant acceleration factors but they do not change the qualitative conclusions (chemical ordering) reached from the data of Table 3. Interestingly, it is seen that the number of atoms involved in the ring connecting the two nitrogen atoms dictates the height of the energy barrier. Lower barriers are found for the 6-membered rings (**4** and **6**), while the geometrical constraints inherent to the ESIPT process appear incompatible with a 4-membered ring (**3**). We also underline that the very low ESIPT barrier of 0.02 eV in molecule **4** which contains a 6-membered ring HB pattern is of the order of previously cited systems encompassing a O-H···N HB,[11] confirming the importance of the geometrical effect. Concerning the 5-

membered ring systems, it appears that shorter N-N distances differences between the N form and the TS correspond to lower energy barriers in the ES. An adjusted squared correlation coefficient of 0.92 was computed for this linear relationship on the basis of species **1a-e** and **2** that all contain 5-membered ring HB. Focusing for example on the effects of the CF_3 substituent on the pyridyl pyrazole molecule (**1c**), we notice that the barrier in the ES increases with respect to **1a** (from 0.36 to 0.39 eV). In a recent experimental study, it was proposed that the acidity of the N-H donor increases due to the presence of a EWG, which in turn lowers the energy barrier.[14] If this explanation holds for the GS, where the presence of the CF_3 substituent lowers the PT barrier by 0.12 eV, our TD-DFT calculations show that it is not the case in the ES. Interestingly this fact is confirmed by the more reliable EOM-CCSD approach, which predicts exactly the same barriers for ESIPT with or without the presence of the CF_3 group (see Table 1). The trend in energy barriers for the ES can however be related to the variations of the N-N distances between the N form and the TS, although we should point out that this relation does not hold for molecule **1f**. We now discuss the molecules containing two substituents. First, we note that adding a second –CF_3 on position 4 of the pyrazole ring decreases the energy barrier for the PT in the GS by 0.18 eV compared to the molecule bearing only one trifluoromethyl group. The difference is only 0.08 eV in the ES. For the species harboring a donor group (–OMe) on the pyridyl ring in *meta* position with respect to the pyrazol (that is, position 8), a slight decrease of 0.07 eV of the energy barrier for the PT in the GS is observed. On the contrary an increase of 0.07 eV is found when the donor group is placed in *para* position (position 9). This difference is understandable since the presence of the donor group in *meta* more strongly increases the electronic density on the nitrogen atom of the pyridyl cycle, and thus its basicity than when the group is located in *para* position. Again, the situation is completely different in the ES where the

ESIPT barriers are similar for both species (0.48 and 0.47 eV for **1e** and **1f** respectively). Computation of density difference plots between ground and excited states in molecules **1a-c** also provide qualitative insights on the influence of substituents. From Fig. 3, it is clear that the substituents have little impact on the electronic density differences. In all of the three molecules, a rather similar transfer of electronic density from the pyrazole to the pyridyl cycle is observed upon excitation. This change is in agreement with the increased basicity of the nitrogen atom of the pyridine moiety that, in turn, explains the stability of the T forms in the ES. The limited impact of substituents on electronic density differences is confirmed by dipole differences between ground and excited states (Table 4). These are indeed similar for the three molecules in all forms (N, T, and TS). We note that they are slightly larger (around 1 D) with the methyl substituent (molecule **1b**). Experimental data[14] are however very similar for **1a** and **1b**, suggesting that the effect of the substituent on the dipole moments should not be considered as a decisive criteria in these dyes.

Table 3 Relative free energies (in eV) between stationary points located on the ground and excited state PES. A positive value indicates a favored N form. All calculations were performed with the M06-2X functional in vacuum. The differences between the distances separating the two nitrogen atoms in the N form and in the TS are given in parentheses (in Å). See Fig. 2 for a description of the parameters.

	ΔG (GS)	$\Delta G^{\ddagger}$ (GS)	ΔG(ES)	$\Delta G^{\ddagger}$ (ES)
1a	1.09	1.31	-0.53	0.36 (-0.313)
1b	1.11	1.30	-0.66	0.28 (-0.292)

1c	0.97	1.21	-0.53	0.39 (-0.325)
1d	0.82	1.03	*-0.49*[b]	0.31 (-0.283)
1e	0.90	1.14	-0.33	0.48 (-0.375)
1f	1.09	1.28	-0.42	0.47 (-0.312)
2	0.85	1.13	-0.63	0.23 (-0.266)
3	0.60	2.75	-1.02	1.92 (-0.208)
4	/ [a]	/ [a]	-0.51	0.02 (-0.200)
5	0.92	1.79	-0.69	0.92 (-0.404)
6	0.60	0.67	0.19	0.33 (-0.342)

[a] No T nor TS forms were located for this molecule, a scan of the PES indicates that the T form is not a true energetic minimum in the GS. [b] This value should be taken cautiously, as we found a small imaginary frequency (-45*i* cm^{-1}) corresponding to an out-of-plane deviation of some atoms of the pyridine ring. This frequency could not be removed even when applying a *verytight* convergence criterion during the optimisation process.

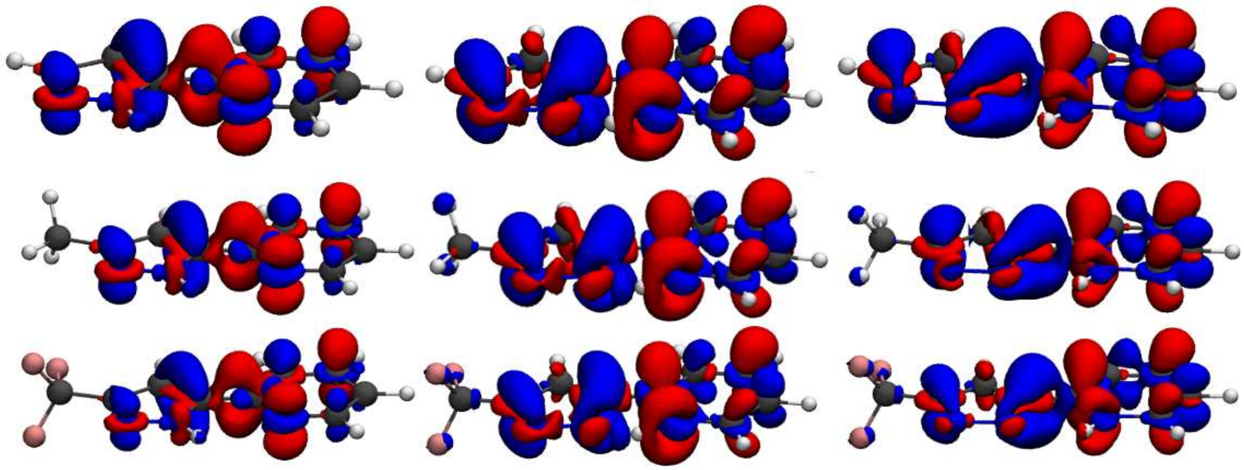

Fig. 3 Electronic density differences between ground and excited states (from left to right: N, TS, and T forms **1a-c**, and from top to down: **1a**, **1b**, **1c**). Red and blue colors respectively represent an increase and a decrease of the electronic density upon photon absorption.

Table 4 Dipole moment differences (in Debye) between the ground and excited states computed in vacuum at the M06-2X/6-311++G(2df,2p) level of theory.

	$\Delta\mu_{GS\text{->}ES}$ N	$\Delta\mu_{GS\text{->} ES}$ TS	$\Delta\mu_{GS\text{->} ES}$ T
1a	3.50	6.14	5.08
1b	3.92	7.12	5.75
1c	2.75	6.20	5.32

Rationalization of substituent effects on optical spectra of pyridyl pyrazole chromophores

As stated in the Introduction, the substituent effects on the absorption and emission spectra of pyridil pyrazole chromophores have recently been studied experimentally by Chou and collaborators.[14] They showed that the presence of a CF_3 group at position 3 induces a dramatic increase of the intensity of the second fluorescence band as well as a large blue-shift compared to the situation without the EWG. Experimental and theoretical spectra for molecules **1a** and **1c** are available in Fig. 4. The explanation given for the change in intensity relied on a faster ESIPT process in **1c** due to the increased acidity of the proton. However, as explained in the previous paragraph, this is not confirmed by theory, the energy barrier for ESIPT being even larger with the trifluoromethyl moiety than with a methyl group. Concerning the shape of the bands, it can be seen in Fig. 4, that simulated vibronic spectra very nicely match the experiments in molecule **1c** for the absorption as well as both N and T emission bands. A small overshooting of absolute energies is observed which is expected with the selected functional.[31,32,34] The simulated spectrum for molecule **1a** is very similar to the one of **1c**, despite a small decrease of the intensity of the T emission band; and thus it differs from the experimental one regarding the second fluorescence band. Comparing the two theoretical spectra, we note a smaller Stoke shift between N absorption and T emission for **1a** (12941 cm^{-1}) than for **1c** (11762 cm^{-1}). This is qualitatively in agreement with the experiment; however quantitatively, the difference is much more important in experiments with Stoke shifts of 18125 and 12504 cm^{-1} for **1a** and **1c**, respectively. The vibration modes contributing to each peak of the vibronic spectrum of the T form were also analyzed. Interestingly, it appears that two modes associated with a large displacement of the transferred proton are responsible for the main contributions of the peak at 410 nm in **1c** spectrum. Short movies illustrating those vibration modes in molecules **1a** and **1c** are provided in Electronic Supplementary Material[†] (ESI). Following the idea presented in Ref. 11, an estimation of the proportion of N and T forms present in solution can be made by comparing the absolute relative intensities of the N and T tautomers obtained through vibronic calculations to the experimental heights of the emission peaks for N and T forms. In the case of **1c**, we find that a N/T proportion of *ca.* 1/2.3 should be present in solution. It suggests that despite the non-negligible energetic barrier of 0.39 eV, the majority of excited molecules still undergoes ESIPT before emission. On the other hand for **1a**, the proportion of N/T species should be *ca.* 4/1 to reproduce the experimental intensities.

In summary, our results strongly suggest ESIPT for **1c**. On the contrary, the very weak emission band (600-700 nm) seen in **1a** could not be reproduce. We can hypothesize the presence of another species in solution, *e.g.*, a protonated species, aggregated or even a contamination of the sample, rather than emission from the T form. The disappearance of the second fluorescence band in absence of the –CF_3 substituent can hardly be attributed to a significant change of the ESIPT barrier (*cf* Table 3) as it was initially proposed by the experimentalists.[14] Another explanation could arise from the presence of a CI after a rotation around the bond connecting the two aromatic cycles, a CI that could be affected by substituent effects. This type of CI has been characterized with theoretical tools in similar systems, for example in molecules **2** and **5** and we redirect the interested readers to this earlier works for more discussion.[17,23,25]

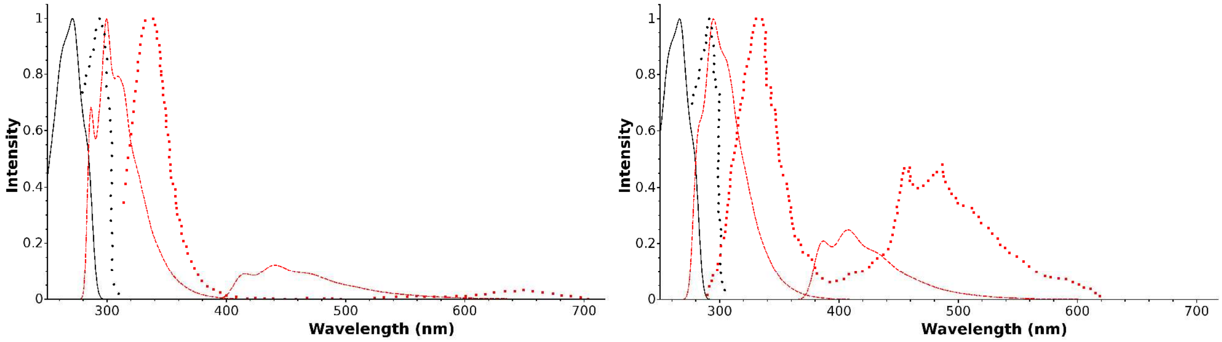

Fig. 4 Comparison between experimental[14] (dots) and theoretical absorption (black) and emission (red, dashed lines) spectra for molecules **1a** (left) and **1c** (right). The normalization of theoretical emission spectra is based on the maximal intensity value obtained in both N and T emissions.

ESIPT in the BFP chromophore analogue

As we have seen in the first section of results, TD-DFT does not provide reliable results for the BFP chromophore analogue (**6**). Indeed, despite predicting a reasonable barrier height for the PT (0.33 eV), the relative stability of N and T forms is not well reproduced by TD-DFT: it predicts a thermodynamically unfavored ESIPT (+0.18 eV) contrary to both experimental evidences and EOM-CCSD results (-0.10 eV). For this reason, the analysis of ESIPT will be done on the basis of EOM-CCSD calculations. In a recent study, Yang and collaborators used TD-DFT to study the same molecule, however no theoretical energetic data were reported in that work.[28] Our EOM-CCSD calculations were carried out with a relatively small atomic basis set, namely 6-31+G(d), due to the expensive computational cost and the poor scaling of the method. However, similar calculations with a larger basis set, 6-311+G(2d,p), have been performed on a simplified molecule **6** where the phenyl and methyl groups were replaced by hydrogen atoms (**6’**). The error of TD-DFT (compared to EOM-CCSD) for the prediction of the relative stability of the two tautomers in the ES is 0.30 eV for **6’**, confirming that TD-DFT fails to satisfactorily describe the PES of the first excited state of this specific molecular pattern.

ESIPT is energetically favored in the BFP chromophore analogue (**6**), the ES T form being indeed more stable than its N counterpart by 0.10 eV whereas the computed energy barrier (0.30 eV) is smaller than the one computed for other systems in which ESIPT was reported (0.50 and 0.33 eV in **1c** and **2**, respectively). Experimentally, the absorption spectrum of **6** shows a band ranging from 350 to 450 nm,[28] the corresponding theoretical wavelength, converted from EOM-CCSD vertical transition energy, is 326 nm. Regarding the emission spectrum, experimentally, there is a first peak (emission of the N form) between 425 and 525 nm followed by a second one (emission of the T form), more intense, in the 550-700 nm range.[28] These values can be compared with the theoretical ones of 395 and 519 nm for the emission of the N and the T form, respectively. In terms of Stoke shifts, values of 3700 and 8330 cm^{-1} are estimated from measurements;[28] and they can be compared to the theoretical ones, 5359 and 11407 cm^{-1}. We thus note that while theory systematically underestimates the observed wavelengths, Stoke shifts are slightly overestimated. Several factors explain these discrepancies between theory and experiment. First, as stated above, the large computational cost of EOM-CCSD required us to use a relatively limited atomic basis set. Then, as geometry optimization and frequency calculations cannot be performed with the selected method, we had to rely on vertical excitations computed on the TD-DFT optimized geometries. Finally, no solvent effect was taken into account in our EOM-CCSD calculations.

Conclusion

In this work, we have investigated the excited state intramolecular proton transfer (ESIPT) in a series of chromophores presenting an N-H···N intramolecular hydrogen bond with both TD-DFT and EOM-CCSD approaches. We first focused on substituent effects in pyridyl pyrazoles (**1a-c**). The selected approach confirmed that the lowering of the energy barrier for the proton transfer in the GS due to the addition of a trifluoromethyl group. But more importantly, it appears that this effect does not pertain in the ES, the computed energy barriers for ESIPT being very similar in **1a-f**. The simulated spectrum for the emission of **1c** matched very well the experimental one, for both tautomers, effectively confirming ESIPT for this species. It was however not the case for **1a**, suggesting that ESIPT is probably not responsible for the tiny, very red-shifted band observed in the emission spectrum of this compound. Further works should be carried out to understand the disappearance of ESIPT fluorescence in absence of a EWG substituent in pyridyl pyrazole derivatives.

For the analogue of the Blue Fluorescent Protein (BFP) chromophore (**6**), it is seen that the selected TD-DFT approach does not perform well compared to both EOM-CCSD data and experimental evidences. This is, to our knowledge, one of the first examples in which the common approximations used in TD-DFT fail to predict reliable ESIPT relative energies. Indeed, TD-DFT predicts a thermodynamically unfavorable ESIPT in this case, the T form being less stable than the N one in the ES. It would be interesting to investigate more structures derived from **6** in order to figure out the reasons behind this TD-DFT weakness.

Acknowledgements

PH thanks the Fund for Scientific Research (FRS-FNRS) for his PhD Fellowship, as well as the Fédération Wallonie Bruxelles for financial support. This research used resources of the Plateforme Technologique de Calcul Intensif (PTCI) (http://www.ptci.unamur.be) located at the University of Namur, Belgium, which is supported by the F.R.S.-FNRS (convention 2.4.617.07.F). The PTCI is a member of the Consortium des Équipements de Calcul Intensif (CECI). DJ indebted to the *Région des Pays de Loire (recrutement sur poste stratégique)* and to the ERC StG program (Grant: Marches – 278845) for financial support. EOM-CCSD calculations used resources of (1) the GENCI-CINES/IDRIS (Grant c2013085117), (2) CCIPL (Centre de Calcul Intensif des Pays de Loire), and (3) a local Troy cluster.

Notes and References

[a] Laboratoire de Physico-Chimie Informatique (PCI), Unité de Chimie Physique Théorique et Structurale, Université de Namur, 61 rue de Bruxelles, 5000 Namur, Belgium.

[b] Laboratoire CEISAM - UMR CNRS 6230, Université de Nantes, 2 rue de la Houssinière, BP92208, 44322 Nantes Cedex 3, France.

[c] Institut Universitaire de France, 103 Boulevard St Michel, 75005 Paris Cedex 5, France.

*Corresponding authors: pierre.hubin@unamur.be, Denis.Jacquemin@univ-nantes.fr

[†] Electronic Supplementary Information (ESI) available: gif movies of vibrational modes in **1a** and **1c** contributing to T emission peak and associated with a large displacement of the transferred proton.

References

1 A. Heller and D. L. Williams, *J Phys Chem*, 1970, **74**, 4473.

2 O. K. Abou-Zied, R. Jimenez, E. H. Z. Thompson, D. P. Millar and F. E. Romesberg, *J Phys Chem A*, 2002, **106**, 3665.

3 S. Park, O.-H. Kwon, S. Kim, S. Park, M.-G. Choi, M. Cha, S. Y. Park and D.-J. Jang, *J Am Chem Soc*, 2005, **127**, 10070.

4 M. J. Paterson, M. A. Robb, L. Blancafort and A. D. DeBellis, *J Phys Chem A*, 2005, **109**, 7527.

5 K.-I. Sakai, T. Tsuzuki, Y. Itoh, M. Ichikawa and Y. Taniguchi, *Appl Phys Lett*, 2005, **86**, 81103.

6 K.-Y. Chen, Y.-M. Cheng, C.-H. Lai, C.-C. Hsu, M.-L. Ho, G.-H. Lee and P.-T. Chou, *J Am Chem Soc*, 2007, **129**, 4534.

7 W.-H. Chen and Y. Pang, *Tetrahedron Lett*, 2010, **51**, 1914.

8 J. Wu, W. Liu, J. Ge, H. Zhang and P. Wang, *Chem Soc Rev*, 2011, **40**, 3483.

9 W. Chen, B. D. Wright and Y. Pang, *Chem Comm*, 2012, **48**, 3824.

10 T. Mutai, H. Sawatani, T. Shida, H. Shono and K. Araki, *J Org Chem*, 2013, **78**, 2482.

11 Y. Houari, A. Charaf-Eddin, A. D. Laurent, J. Massue, R. Ziessel, G. Ulrich and D. Jacquemin, *Phys Chem Chem Phys*, 2014, **16**, 1319.

12 W.-S. Yu, C.-C. Cheng, Y.-M. Cheng, P.-C. Wu, Y.-H. Song, Y. Chi and P.-T. Chou, *J Am Chem Soc*, 2003, **125**, 10800.

13 M.-W. Chung, J.-L. Liao, K.-C. Tang, C.-C. Hsieh, T.-Y. Lin, C. Liu, G.-H. Lee, Y. Chi and P.-T. Chou, *Phys Chem Chem Phys*, 2012, **14**, 9006.

14 T.-Y. Lin, K.-C. Tang, S.-H. Yang, J.-Y. Shen, Y.-M. Cheng, H.-A. Pan, Y. Chi and P.-T. Chou, *J Phys Chem A*, 2012, **116**, 4438.

15 V. Vetokhina, K. Dobek, M. Kijak, I. I. Kamińska, K. Muller, W. R. Thiel, J. Waluk and J. Herbich, *ChemPhysChem*, 2012, **13**, 3661.

16 M. Kijak, Y. Nosenko, A. Singh, R. P. Thummel and J. Waluk, *J Am Chem Soc*, 2007, **129**, 2738.

17 M. F. Rode and A. L. Sobolewski, *Chem Phys*, 2008, **347**, 413.

18 C. A. Taylor, M. A. El-Bayoumi and M. Kasha, *Proc Natl Acad Sci*, 1969, **63**, 253.

19 L. Serrano-Andrés, M. Merchán, A. C. Borin and J. Stålring, *Int J Quantum Chem*, 2001, **84**, 181.

20 R. Casadesús, M. Moreno and J. M. Lluch, *Chem Phys*, 2003, **290**, 319.

21 L. Serrano-Andrés and M. Merchán, *Chem Phys Lett*, 2006, **418**, 569.

22 H. Fang and Y. Kim, *J Chem Theory Comput*, 2013, **9**, 3557.

23 A. L. Sobolewski and W. Domcke, *J Phys Chem A*, 2007, **111**, 11725.

24 Y. Nosenko, G. Wiosna-Sałyga, M. Kunitski, I. Petkova, A. Singh, W. J. Buma, R. P. Thummel, B. Brutschy and J. Waluk, *Angew Chem Int Ed*, 2008, **47**, 60037.

25 L. Spörkel, G. Cui, A. Koslowski and W. Thiel, *J Phys Chem A*, 2013, **118**, 152.

26 A. Kyrychenko, J. Herbich, M. Izydorzak, F. Wu, R. P. Thummel and J. Waluk, *J Am Chem Soc*, 1999, **121**, 11179.

27 A. Kyrychenko and J. Waluk, *J Phys Chem A*, 2006, **110**, 11958.

28 X. Fang, Y. Wang, D. Wang, G. Zhao, W. Zhang, A. Ren, H. Wang, J. Xu, B.-R. Gao and W. Yang, *J Phys Chem Lett*, 2013, **5**, 92.

29 Gaussian 09, Revision D.01, M. J. Frisch, G. W. Trucks, H. B. Schlegel, G. E. Scuseria, M. A. Robb, J. R. Cheeseman, G. Scalmani, V. Barone, B. Mennucci, G. A. Petersson, H. Nakatsuji, M. Caricato, X. Li, H. P. Hratchian, A. F. Izmaylov, J. Bloino, G. Zheng, J. L. Sonnenberg, M. Hada, M. Ehara, K. Toyota, R. Fukuda, J. Hasegawa, M. Ishida, T. Nakajima, Y. Honda, O. Kitao, H. Nakai, T. Vreven, J. A. Montgomery, Jr., J. E. Peralta, F. Ogliaro, M. Bearpark, J. J. Heyd, E. Brothers, K. N. Kudin, V. N. Staroverov, R. Kobayashi, J. Normand, K. Raghavachari, A. Rendell, J. C. Burant, S. S. Iyengar, J. Tomasi, M. Cossi, N. Rega, J. M. Millam, M. Klene, J. E. Knox, J. B. Cross, V. Bakken, C. Adamo, J. Jaramillo, R. Gomperts, R. E. Stratmann, O. Yazyev, A. J. Austin, R. Cammi, C. Pomelli, J. W. Ochterski, R. L. Martin, K. Morokuma, V. G. Zakrzewski, G. A. Voth, P. Salvador, J. J. Dannenberg, S. Dapprich, A. D. Daniels, Ö. Farkas, J. B. Foresman, J. V. Ortiz, J. Cioslowski, and D. J. Fox, Gaussian, Inc., Wallingford CT, 2009.

30 Y. Zhao and D. G. Truhlar, *Theor. Chem. Acc.*, 2007, **120**, 215.

31 M. Isegawa, R. Peverati and D. G. Truhlar, *J Chem Phys*, 2012, **137**, 244104.

32 D. Jacquemin, A. Planchat, C. Adamo and B. Mennucci, *J Chem Theory Comput*, 2012, **8**, 2359.

33 S. S. Leang, F. Zahariev and M. S. Gordon, *J Chem Phys*, 2012, **136**, 104101.

34 A. Charaf-Eddin, A. Planchat, B. Mennucci, C. Adamo and D. Jacquemin, *J Chem Theory Comput*, 2013, **9**, 2749.

35 J. Tomasi, B. Mennucci and R. Cammi, *Chem Rev*, 2005, **105**, 2999.

36 R. Cammi, S. Corni, B. Mennucci and J. Tomasi, *J Chem Phys*, 2005, **122**, 104513.

37 M. Caricato, B. Mennucci, J. Tomasi, F. Ingrosso, R. Cammi, S. Corni and G. Scalmani, *J Chem Phys*, 2006, **124**, 124520.

38 F. Santoro, R. Improta, A. Lami, J. Bloino and V. Barone, *J Chem Phys*, 2007, **126**, 84509.

39 F. Santoro, A. Lami, R. Improta and V. Barone, *J Chem Phys*, 2007, **126**.

40 F. Santoro, V. Barone and R. Improta, *J Comput Chem*, 2008, **29**, 957.

41 G. Wiosna, I. Petkova, M. S. Mudadu, R. P. Thummel and J. Waluk, *Chem Phys Lett*, 2004, **400**, 379.

42 O.-H. Kwon, Y.-S. Lee, H. J. Park, Y. Kim and D.-J. Jang, *Angew Chem Int Ed*, 2004, **43**, 5792.